

Bound States in the Continuum in Compact Acoustic Resonators

Ilya Deriy,^{*} Ivan Toftul, Mihail Petrov, and Andrey Bogdanov[†]

Department of Physics and Engineering, ITMO University, 191002, St. Petersburg, Russia

(Dated: November 7, 2021)

We reveal that finite-size solid acoustic resonators can support genuine bound states in the continuum (BICs) completely localized inside the resonator. The developed theory provides the multipole classification of such BICs in the resonators of various shapes. It is shown how breaking of the resonator's symmetry turns BICs into quasi-BICs manifesting themselves in the scattering spectra as high-Q Fano resonances. We believe that the revealed novel states will push the performance limits of acoustic devices and will serve as high-Q building blocks for acoustic sensors, antennas, and topological acoustic structures.

Bound states in the continuum (BICs) are the non-radiating states of an open system with a spectrum embedded in the continuum of the radiating modes of the surrounding space [1]. BICs were firstly predicted in quantum mechanics by von Neumann and Wigner in 1929 [2] but shortly after they were extended to the wave equations in general as their specific solutions. As a result, BICs were found in various fields of physics such as atomic physics, hydrodynamics, and acoustics [3–5]. The zero radiative losses leads to diverging radiative quality factor (Q-factor) making BICs extremely prospective for the energy localisation and enhancement of the incident fields. Since recently, these unique properties of BICs have been actively utilized in photonics, where they have already proven themselves as an effective platform for lasing, polaritonic, sensing, and optical harmonic generation applications [6–11].

Decoupling the the resonance from all open scattering channels one can obtain a genuine BIC, which becomes possible only if the number of the adjusting parameters is more than the number of the scattering channels. A typical example of a system with the finite number scattering channels is a resonator coupled to one or several waveguide modes [12–14]. Alternatively, a finite number of the scattering channels may exist in infinite periodic structures [15, 16]. For finite size structures the number of scattering channels is infinite, and the existence of BICs in such systems is prohibited by *non-existence theorem* [1]. The only exception is the structures surrounded by a completely opaque shell providing decoupling of the internal resonances from the outside radiation continuum, which in quantum mechanics corresponds to an infinite high potential barriers, in acoustics to hard-wall boundaries, and in optics to perfect conducting walls or epsilon-near-zero barriers [17, 18]. Finding of a genuine BIC in compact systems is a challenging fundamental problem, and its solution would make possible the implementation of subwavelength high-Q resonators having broad range of potential applications.

In this letter, a backdoor in the 'non-existence theorem' is revealed. While BICs are prohibited in finite photonic and quantum mechanical systems, we show that acoustics is relieved of these constraints. We propose a

genuine acoustic BIC in compact solid resonators placed in nonviscous fluids (gas or liquid). The origin of the unexplored BICs is illustrated in Fig. 1. In acoustics, in contrast to photonics and quantum mechanics, there are two types of waves: (i) *pressure waves* with longitudinal polarization ($\mathbf{u} \parallel \mathbf{k}$) and (ii) *shear waves* with transversal polarization ($\mathbf{u} \perp \mathbf{k}$) [19]. Here, \mathbf{u} is the displacement vector and \mathbf{k} is the wave vector. While in solids, both waves coexist, nonviscous fluids host only pressure waves which are longitudinal. In general case of an arbitrary shaped solid resonator, all the eigenmodes are hybrid containing longitudinal and transverse components hybrid and, thus, are coupled to the radiation continuum. However, one can find specific shapes of the resonators allowing purely torsion modes which displacement is tangential at each point of the resonator boundary. The torsion oscillations do not produce pressure on the surrounding fluid being completely decoupled from the radiation continuum. Their energy remains perfectly confined inside the resonator forming ideal genuine acoustic BICs.

We may designate the proposed non-radiating states as *polarization-protected acoustic BICs* as they are possible exclusively due to the fact that non-viscous fluids support longitudinal waves only, while solids host both longitudinal and transversal waves. Due to similar rea-

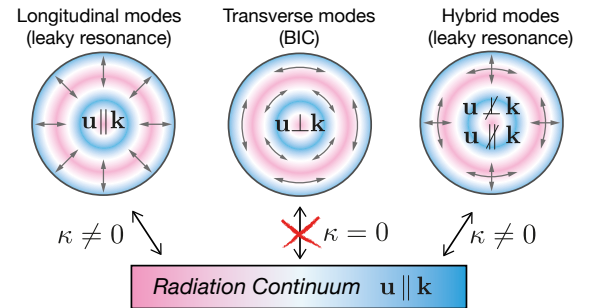


FIG. 1. Polarization of eigenmodes in a solid acoustic resonator. The transversal modes ($\mathbf{u} \perp \mathbf{k}$) do not coupled to the radiation continuum forming a bound state in the continuum. Here, κ is the coupling coefficient, \mathbf{u} is the displacement vector, and \mathbf{k} is the wave vector.

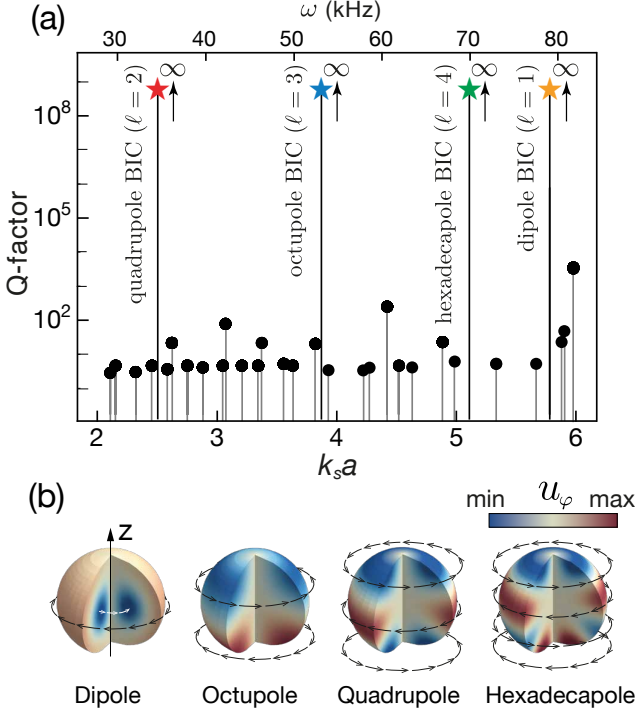


FIG. 2. Polarization-protected BICs in a solid spherical resonator. (a) Spectrum and radiative Q-factor of the resonator. Parameters of the resonator are mentioned in the text. (b) Distributions of the azimuthal component of the displacement (u_φ) for the dipole, quadrupole, octupole, and hexadecapole BICs with $m = 0$.

sons, the shear modes in a solid slab appear to be non-radiating [20]. To be frank, BICs in compact resonators can exist even in optics, for example, in the form of the radial plasmonic oscillations in a metal spherical particle at the plasma frequency. In this case, the longitudinal plasmonic oscillations are not coupled to the far-field electromagnetic radiation which is purely transversal. However, the observation of these modes is hindered due to high losses in plasmonic nanostructures.

We start with considering a problem of eigen modes in a rigid sphere of radius a in order to show rigorously that the polarization-protected BICs exist in compact resonators. We assume that the sphere is made of a solid isotropic material surrounded by gas or fluid environment. The displacement field $\mathbf{u}(\mathbf{r})$ inside and outside the sphere obeys the Helmholtz equation [19]

$$\Delta \mathbf{u}_i^j(\mathbf{r}) + (k_i^j)^2 \mathbf{u}_i(\mathbf{r}) = 0. \quad (1)$$

Here, the lower index $i = s, p$ encodes the displacements of shear or pressure waves respectively, the upper index $j = \{\text{in, out}\}$ corresponds to the fields inside and outside of the resonator respectively, $k_i^j = \omega/c_i^j$ is the wavevector, and c_i^j is the velocity of displacement waves. The boundary conditions at the surface of a solid sphere placed

in gas or fluid can be written in spherical coordinates (r, θ, φ) as follows [21]:

$$\sigma_{rr}^{\text{in}} = -p^{\text{out}}, \quad \sigma_{r\theta}^{\text{in}} = 0, \quad \sigma_{r\varphi}^{\text{in}} = 0, \quad u_r^{\text{in}} = u_r^{\text{out}}, \quad (2)$$

where $\sigma_{ij} = \lambda \delta_{ij} \text{Tr} \hat{\varepsilon} + \mu \varepsilon_{ij}$ is the Cauchy stress tensor, $2\hat{\varepsilon} = [\nabla \mathbf{u} + (\nabla \mathbf{u})^T]$ is the strain tensor, p^{out} is the gas pressure, which is connected to the displacement field as $\rho^{\text{out}} \omega^2 \mathbf{u}^{\text{out}} = \nabla p^{\text{out}}$ (see Supplemental Material for details). We also assume that outside the sphere the solution has a form of the outgoing waves. Based on that, the solutions of the vector Helmholtz equation(1) can be written in terms of the vector spherical harmonics [4]

$$\mathbf{u}^j(\mathbf{r}) = \sum_{\ell m} a_{\ell m}^j \mathbf{M}_{\ell m}(\mathbf{r}, k_s^j) + b_{\ell m}^j \mathbf{N}(\mathbf{r}, k_s^j) + c_{\ell m}^j \mathbf{L}_{\ell m}(\mathbf{r}, k_p^j). \quad (3)$$

Here, $\ell = 0, 1, 2, \dots$ is the total angular momentum quantum number and $m = 0, \pm 1, \dots, \pm \ell$ is the projection of the angular momentum on the z -axis (magnetic quantum number) [see Fig. 2(b)]. While outside the cavity one should put $a_{\ell m}^{\text{out}} = b_{\ell m}^{\text{out}} = 0$ for all ℓ and m as fluid(gas) supports only longitudinal waves, inside the cavity one should account for all the vector harmonics. As a result, the homogeneous system of equations on the expansion coefficients can be obtained

$$\hat{\mathbf{D}}_{\ell m} \mathbf{f}_{\ell m} = 0, \quad (4)$$

where vector $\mathbf{f}_{\ell m} = [a_{\ell m}^{\text{in}}, b_{\ell m}^{\text{in}}, c_{\ell m}^{\text{in}}, c_{\ell m}^{\text{out}}]^T$ is the vector of coefficients, and $\hat{\mathbf{D}}_{\ell m} = \text{diag}[\hat{\mathbf{D}}_{\ell m}^{1 \times 1}, \hat{\mathbf{D}}_{\ell m}^{3 \times 3}]$ is a block-diagonal matrix with the explicit form provided in Supplemental Material. In virtue of the block-diagonal form of $\hat{\mathbf{D}}_{\ell m}$, the equation on eigenfrequencies is factorized:

$$\underbrace{\det \hat{\mathbf{D}}_{\ell m}^{1 \times 1}}_{\text{BIC}} \cdot \underbrace{\det \hat{\mathbf{D}}_{\ell m}^{3 \times 3}}_{\text{Rad. modes}} = 0. \quad (5)$$

Generally, the eigen frequency can be rescaled by the factor of c_s/a . However, to have an illustrative physical example we will use the secondary frequency axis corresponding to the sphere of radius $a = 5$ cm placed in air with density $\rho_0 = 1.23 \text{ kg/m}^3$. The density of the material of the sphere equals to $\rho = 10\rho_0$, while the velocity of shear and pressure waves are taken equal to $c_s = 2c_0$, $c_p = 3c_0$, respectively, where $c_0 = 343 \text{ m/s}$ is the velocity of sound in the air.

The spectrum of the resonator (eigenfrequencies and Q-factors) obtained from numerical solution of Eq. (5) is shown in Fig. 2(a). It consist of radiative modes and BICs with infinitely high radiative Q-factors. One can show that purely real eigenfrequencies corresponding to BICs satisfy the equation $\det \hat{\mathbf{D}}_{\ell m}^{1 \times 1} = 0$, which can be

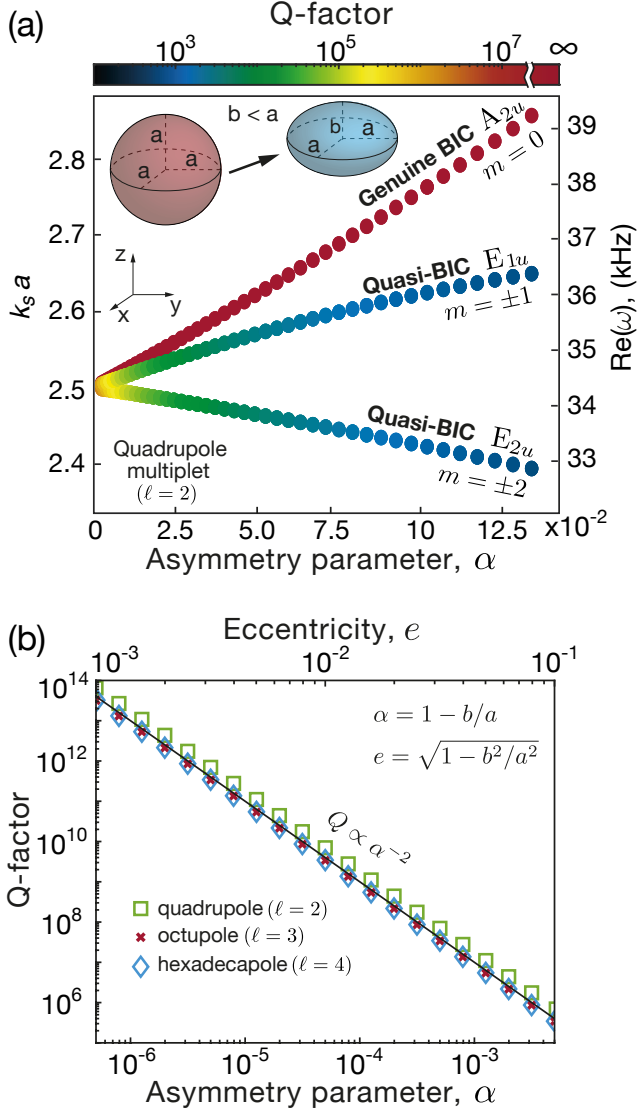


FIG. 3. Splitting of a quadrupole multiplet into BIC and quasi-BIC in a solid spheroid. (a) Frequency shift and Q-factors versus asymmetry parameter $\alpha = 1 - b/a$. (b) Dependence of the Q-factor on the asymmetry parameter α for quadrupole, octupole, and hexadecapole quasi-BICs with $m = \pm 2$.

written explicitly as follows (see Supplemental Material for details):

$$(1 - \ell)j_\ell(x) + xj_{\ell+1}(x) = 0. \quad (6)$$

Here $j_\ell(x)$ is the spherical Bessel function, and $x = k_s a$. Due to spherical symmetry of the problem, the obtained equation does not depend on m , therefore, the its solution is $(2\ell + 1)$ -fold degenerate. The table containing the roots of Eq. (6) is provided in Supplemental Material.

It also follows from Eqs. (4) and (5) that $b_{\ell m}^{\text{in}} = c_{\ell m}^{\text{in}} = c_{\ell m}^{\text{out}} = 0$ for BICs and, consequently, the displacement field \mathbf{u} contains only vector harmonics $\mathbf{M}_{\ell m}$ and they are

completely localized inside the resonator. Indeed, $\mathbf{M}_{\ell m}$ harmonics correspond to the torsion oscillations which totally lack of radial components in sharp contrast to $\mathbf{L}_{\ell m}$ and $\mathbf{N}_{\ell m}$ and, thus, can not excite pressure waves in the surrounding fluids. The distribution of the displacement field for BICs with $m = 0$ and $\ell = 1, 2, 3, 4$ is shown in Fig. 2(b). In the light of the modes structure, we should note that Eq. (6) can be also obtained from Eq. (1) applying stress-free boundary conditions [23, 24].

A curious fact deserving special attention is that the fundamental acoustic BIC in a solid sphere is a quadrupole mode ($\ell = 2$) rather than a dipole. This fact can be understood intuitively: the time-average angular momentum of the resonator should be zero, i.e. the resonator should not rotate as a whole. For the dipole modes, the external and internal layers oscillate in anti-phase compensating the rotation [see Fig. 2(b)], and it results in a quite large radial wavenumber $k_s a \approx 5.8$. For the quadrupole mode $k_s a \approx 2.5$ and the oscillation phase does not change along the radial direction. Thus, the time-average angular momentum is compensated by anti-phase oscillations of the upper and lower hemispheres [see Fig. 2(b)].

A BIC according to its definition is completely decoupled from all propagating waves of the surrounding space, and, thus, it cannot be excited from the far-field by pressure waves. However, the excitation is possible by near-field sources or due to nonlinear effects [25–27]. Another efficient method, that is the most used in practice, is based on introduction of small coupling between the BIC and radiative modes. Therefore, a genuine BIC turns into a *quasi-BIC* (q-BIC) – a high-Q state that manifests itself in the scattering spectrum as a narrow Fano resonance [28]. Recently, the q-BICs were suggested as very promising candidates for sensing, lasing, and nonlinear optics applications [11, 29–34].

In order to show how a genuine acoustic BIC turns into a q-BIC, we slightly deform the spherical resonator of radius a into an oblate spheroid with the semi-axes a and b [see inset in Fig. 3(a)]. The dependence of the resonant frequency and Q-factor for the quadrupole BIC ($\ell = 2$) on the asymmetry parameter $\alpha = 1 - a/b$ is shown in Fig. 3(a). As it was mentioned above, the BICs in spherical resonator are $(2\ell + 1)$ -fold degenerate multiplets. In the spheroid, this multiplet splits into one singlet state corresponding to the BIC and 2ℓ of two-fold degenerate doublet q-BICs (see Supplemental Material for details) [Fig. 3(a)]. The Q-factor of the q-BICs drops quadratically with the asymmetry parameter α [see Fig. 3(b)] that completely agrees with the general theory of q-BICs [28].

In terms of the group theory, the quadrupole BIC in a spheroid ($D_{\infty h}$ symmetry) corresponds to one-dimensional irreducible representation (irrep) A_{2u} , and the doublets of q-BICs correspond to two-dimensional irreps E_{1u} and E_{2u} . The degeneracy of the q-BICs remains due to the rotational symmetry of the spheroid,

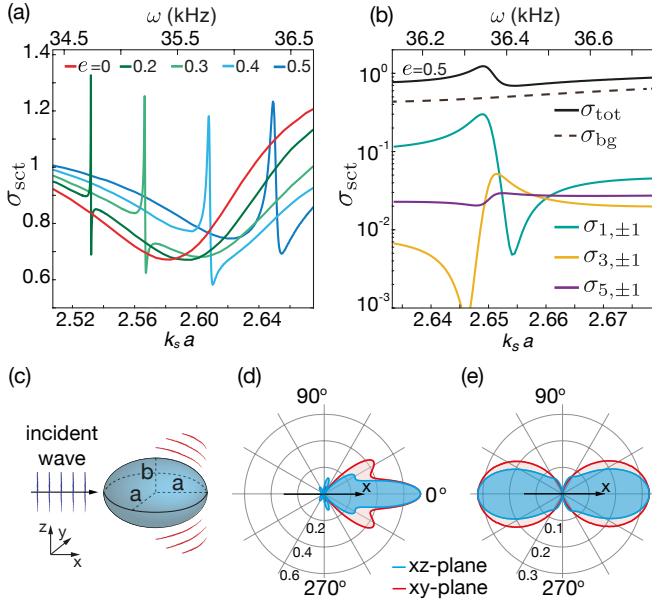


FIG. 4. (a) Spectrum of scattering efficiency of a solid spheroid calculated for various eccentricities e . (b) Spectrum of the total and partial scattering efficiencies calculated near q-BIC (E_{1u}) for $e = 0.5$. (c) The excitation scheme. (d) Directivity patterns of the total scattered field and (e) scattered field accounted for the resonant contribution of q-BIC only. The diagrams are plotted for $e = 0.1$ at the resonant frequency of q-BIC ($k_s a = 2.51$).

thus, the doublet can be associated with clockwise- and counterclockwise rotational modes. Following Ref. [5] we can write the multipole series of the BICs and q-BICs, and selection rules for their excitation by a plane pressure wave incident from different directions (see Table I). The survivor BICs in a spheroid are contributed only by the vector harmonics $\mathbf{M}_{\ell m}$ with even ℓ and $m = 0$. As a spheroid has a symmetry plane (xy), there is a second series of genuine BICs contributed by the vector harmonics $\mathbf{M}_{\ell m}$ with odd ℓ and $m = 0$ (see Supplemental Material for details).

One may see from Table I that q-BICs from E_{1u} can be excited by a plane pressure wave propagating along the x - or y -axis. The q-BICs from E_{2u} can be excited only at oblique incidence. Indeed, the excitation from the x -, y - directions is forbidden due to inconsistency between the parity of the mode and the incident wave, and the excitation from the z -direction is forbidden due to the fact that the incident wave contains only the harmonics with $m = 0$.

Figure 4(a) shows the scattering efficiency σ_{sct} (scattering cross-section normalized to the geometric cross-section) of a solid spheroid excited by a plane pressure wave propagating along the x -axis. The scheme of excitation is illustrated in Fig. 4(c). The spectra for different eccentricities e were calculated numerically using COMSOL Multiphysics. One can see that q-BIC correspond-

TABLE I. Splitting of a quadrupole multiplet BIC ($\ell = 2$) in a spheroid. Multipole content of the modes and selection rules for their excitation by a plane wave.

Irrep	Mode	Multipoles	Excitation along x or y	Excitation along z
A_{2u}	BIC	$\mathbf{M}_{2,0}, \dots, \mathbf{M}_{2s,0}$	No	No
E_{1u}	q-BIC	$\mathbf{L}_{1,\pm 1}, \dots, \mathbf{L}_{2s+1,\pm 1}$ $\mathbf{N}_{1,\pm 1}, \dots, \mathbf{N}_{2s+1,\pm 1}$ $\mathbf{M}_{2,\pm 1}, \dots, \mathbf{M}_{2s,\pm 1}$	Yes	No
E_{2u}	q-BIC	$\mathbf{L}_{3,\pm 2}, \dots, \mathbf{L}_{2s+1,\pm 2}$ $\mathbf{N}_{3,\pm 2}, \dots, \mathbf{N}_{2s+1,\pm 2}$ $\mathbf{M}_{2,\pm 2}, \dots, \mathbf{M}_{2s,\pm 2}$	No	No

ing to irrep E_{1u} appears as a high-Q Fano resonance that collapses when e tends to zero manifesting the formation of a genuine BIC. Figure 4(b) shows the contribution of the resonant and non-resonant scattering channels $\sigma_{\ell m}$ to the total scattering efficiency σ_{tot} . Figures 4(d) and 4(e) show the directivity patterns for the total scattered field and scattered field accounted for only the resonant harmonics of q-BIC (see Table I). The diagrams are plotted for the spheroid with $e = 0.1$ at the resonant frequency of q-BIC ($k_s a = 2.51$). One can see that the q-BIC behaves as dipole in the far-field but the non-resonant scattering drastically changes the directivity pattern.

As we see from Fig. 3(a), the polarization-protected acoustic BICs exist not only in a sphere but also in a spheroid. A reasonable question is 'Can we find all possible shapes of resonators capable of supporting such BICs?'. To answer this question one can address to group theory. Table I shows that the symmetry breaking results in mixing multipoles and each eigenmode represents an infinite series of multipoles. Thus, in the general case of an arbitrary shape resonator, all the modes are radiative. However, the multipole mixing occurs according to the selection rules defined by the symmetry group of the resonator. BICs will survive under reduction of resonator's symmetry if the multipoles $\mathbf{M}_{\ell m}$ do not couple with $\mathbf{N}_{\ell m}$ and $\mathbf{L}_{\ell m}$. Thus, BICs are allowed only if the symmetry group of the resonator contains the irreducible representations with a basis forming by the harmonics $\mathbf{M}_{\ell m}$ only. One can show that such a requirement is fulfilled only for the symmetry groups containing the infinite-fold rotation axis. These are $D_{\infty h}$ (cylinder, spheroid, dimer or linear chain of identical equidistant spheres or cylinders) and $D_{\infty v}$ (cone or an arbitrary body of revolution without horizontal symmetry plane).

In this prospective, a special attention should be paid to the polarization-protected acoustic BICs in a solid cylinder of radius a and height h . Though the eigenvalue problem for an open cylindrical resonator cannot be solved analytically since the variables can not be separated, it becomes possible for particular BIC solution. Indeed, BICs are perfectly localized inside the resonator, thus, the system can be considered as a closed one.

Therefore, the eigenfrequencies can be calculated analytically even in the cylindrical geometry using the stress-free boundary conditions: $(\omega/c_s)^2 = (\alpha_n/a)^2 + (\pi q/h)^2$. Here α_n is the n 'th root of the Bessel function $J_2(x)$, and q is an integer.

The total Q-factor (Q_{tot}) of acoustic BICs is limited by the absorption Q-factor (Q_{abs}) that is defined by the attenuation of shear waves in real materials. For example, the longitudinal loss factor $\eta = E''/E'$ of steel is reported to be on the order of $10^{-4} - 10^{-5}$ [36, 37], where $E = E' + iE''$ is the complex Young modulus. Loss factor of the same order is reported for different ceramics and glasses [36], while for silica the loss factor is on the order of 10^{-6} . Since the longitudinal and shear loss factors are of the same order [38], one can expect the total Q-factor of BICs in real materials to be of the order of $Q = 1/\eta \sim 10^4$ to 10^6 .

In conclusion, we have revealed that genuine acoustic bound states in the continuum may exist in compact solid resonators with a rotational symmetry placed in gas or nonviscous fluid environment. The predicted states are possible due to polarization mismatch between the shear waves in solid resonator and pressure waves in the surrounding media. We believe that our findings are an important step in the development of high-Q resonant acoustics, and the revealed novel BICs in compact structures will serve as building blocks for acoustic antennas, high-sensitive acoustic sensors, and topological acoustic structures.

The authors thank K. Frizyuk, K. Koshelev, and Yu. Kivshar for useful discussions and suggestions. The work is support by the Russian Science Foundation (project #20-72-10141). A.B. acknowledges a support from the "BASIS" Foundation.

* ilya.deriya@metalab.itmo.ru

† a.bogdanov@metalab.itmo.ru

- [1] C. W. Hsu, B. Zhen, A. D. Stone, J. D. Joannopoulos, and M. Soljačić, Bound states in the continuum, *Nat. Rev. Mater.* **1**, 1 (2016).
- [2] J. von Neuman and E. Wigner, On some peculiar discrete eigenvalues, *Phys. Z.* **30**, 465 (1929).
- [3] L. Fonda, Bound states embedded in the continuum and the formal theory of scattering, *Ann. Phys.* **22**, 123 (1963).
- [4] F. Ursell, Trapping modes in the theory of surface waves, in *Proc. Camb. Phil. Soc.*, Vol. 47 (1951) pp. 347–358.
- [5] R. Parker, Resonance effects in wake shedding from parallel plates: some experimental observations, *J. Sound Vib.* **4**, 62 (1966).
- [6] S. I. Azzam and A. V. Kildishev, Photonic bound states in the continuum: From basics to applications, *Adv. Opt. Mater.* **9**, 2001469 (2021).
- [7] K. Koshelev, G. Favraud, A. Bogdanov, Y. Kivshar, and A. Fratalocchi, Nonradiating photonics with resonant dielectric nanostructures, *P. Soc. Photo-opt. Ins.* **8**, 725 (2019).
- [8] A. Kodigala, T. Lepetit, Q. Gu, B. Bahari, Y. Fainman, and B. Kanté, Lasing action from photonic bound states in continuum, *Nature* **541**, 196 (2017).
- [9] K. Koshelev, S. Kruk, E. Melik-Gaykazyan, J.-H. Choi, A. Bogdanov, H.-G. Park, and Y. Kivshar, Subwavelength dielectric resonators for nonlinear nanophotonics, *Science* **367**, 288 (2020).
- [10] V. Kravtsov, E. Khestanova, F. A. Benimetskiy, T. Ivanova, A. K. Samusev, I. S. Sinev, D. Pidgayko, A. M. Mozharov, I. S. Mukhin, M. S. Lozhkin, *et al.*, Nonlinear polaritons in a monolayer semiconductor coupled to optical bound states in the continuum, *Light Sci. Appl.* **9**, 1 (2020).
- [11] A. Tittl, A. Leitis, M. Liu, F. Yesilkoy, D.-Y. Choi, D. N. Neshev, Y. S. Kivshar, and H. Altug, Imaging-based molecular barcoding with pixelated dielectric metasurfaces, *Science* **360**, 1105 (2018).
- [12] T. Lepetit and B. Kanté, Controlling multipolar radiation with symmetries for electromagnetic bound states in the continuum, *Phys. Rev. B* **90**, 241103 (2014).
- [13] A. Pilipchuk, A. Pilipchuk, and A. Sadreev, Bound states in the continuum in open spherical resonator, *Phys. Scripta* **95**, 085002 (2020).
- [14] A. Lyapina, D. Maksimov, A. Pilipchuk, and A. Sadreev, Bound states in the continuum in open acoustic resonators, arXiv preprint arXiv:1506.07107 (2015).
- [15] C. W. Hsu, B. Zhen, J. Lee, S.-L. Chua, S. G. Johnson, J. D. Joannopoulos, and M. Soljačić, Observation of trapped light within the radiation continuum, *Nature* **499**, 188 (2013).
- [16] Z. Sadrieva, M. Belyakov, M. Balezin, P. Kapitanova, E. Nenasheva, A. Sadreev, and A. Bogdanov, Experimental observation of a symmetry-protected bound state in the continuum in a chain of dielectric disks, *Phys. Rev. A* **99**, 053804 (2019).
- [17] F. Monticone and A. Alu, Embedded photonic eigenvalues in 3d nanostructures, *Phys. Rev. Lett.* **112**, 213903 (2014).
- [18] I. Liberal and N. Engheta, Nonradiating and radiating modes excited by quantum emitters in open epsilon-near-zero cavities, *Sci. Adv.* **2**, e1600987 (2016).
- [19] L. E. Kinsler, A. R. Frey, A. B. Coppers, and J. V. Sanders, *Fundamentals of Acoustics*, 4th ed. (John Wiley & Sons, New York, 1999).
- [20] I. Quotane, B. Djafari-Rouhani, *et al.*, Trapped-mode-induced fano resonance and acoustical transparency in a one-dimensional solid-fluid phononic crystal, *Phys. Rev. B* **97**, 024304 (2018).
- [21] M. A. Isakovich, *General Acoustics* (Nauka, Moscow, 1973).
- [4] C. F. Bohren and D. R. Huffman, *Absorption and Scattering of Light by Small Particles* (John Wiley & Sons, New York, 2008).
- [23] A. Tamura, K. Higeta, and T. Ichinokawa, Lattice vibrations and specific heat of a small particle, *J. Phys. C: Solid State Phys.* **15**, 4975 (1982).
- [24] S. Tamim and J. Bostwick, The elastic rayleigh drop, *Soft Matter* **15**, 9244 (2019).
- [25] E. Bulgakov, K. Pichugin, and A. Sadreev, All-optical light storage in bound states in the continuum and release by demand, *Opt. Express* **23**, 22520 (2015).
- [26] A. Chukhrov, S. Krasikov, A. Yulin, and A. Bogdanov, Excitation of a bound state in the continuum via spontaneous symmetry breaking, arXiv preprint

- arXiv:2101.05669 (2021).
- [27] L. Yuan and Y. Y. Lu, Excitation of bound states in the continuum via second harmonic generations, *Siam J. Appl. Math.* **80**, 864 (2020).
- [28] K. Koshelev, S. Lepeshov, M. Liu, A. Bogdanov, and Y. Kivshar, Asymmetric metasurfaces with high-q resonances governed by bound states in the continuum, *Phys. Rev. Lett.* **121**, 193903 (2018).
- [29] K. Koshelev, A. Bogdanov, and Y. Kivshar, Meta-optics and bound states in the continuum, *Sci. Bull.* **64**, 836 (2019).
- [30] K. Koshelev, Y. Tang, K. Li, D.-Y. Choi, G. Li, and Y. Kivshar, Nonlinear metasurfaces governed by bound states in the continuum, *ACS Photonics* **6**, 1639 (2019).
- [31] Z. Liu, Y. Xu, Y. Lin, J. Xiang, T. Feng, Q. Cao, J. Li, S. Lan, and J. Liu, High-q quasibound states in the continuum for nonlinear metasurfaces, *Phys. Rev. Lett.* **123**, 253901 (2019).
- [32] A. Leitis, A. Tittl, M. Liu, B. H. Lee, M. B. Gu, Y. S. Kivshar, and H. Altug, Angle-multiplexed all-dielectric metasurfaces for broadband molecular fingerprint retrieval, *Sci. Adv.* **5**, eaaw2871 (2019).
- [33] A. Vaskin, R. Kolkowski, A. F. Koenderink, and I. Staude, Light-emitting metasurfaces, *Nanophotonics* **8**, 1151 (2019).
- [34] M. Liu and D.-Y. Choi, Extreme huygens' metasurfaces based on quasi-bound states in the continuum, *Nano Lett.* **18**, 8062 (2018).
- [5] S. Gladyshev, K. Frizyuk, and A. Bogdanov, Symmetry analysis and multipole classification of eigenmodes in electromagnetic resonators for engineering their optical properties, *Phys. Rev. B* **102**, 075103 (2020).
- [36] J. Zhang, R. Perez, and E. Lavernia, Documentation of damping capacity of metallic, ceramic and metal-matrix composite materials, *J. Mater. Sci.* **28**, 2395 (1993).
- [37] T. Irvine, Damping properties of materials, *Magnesium* **5000**, 10 (2004).
- [38] T. Pritz, Relation of bulk to shear loss factor of solid viscoelastic materials, *J. Sound Vib.* **324**, 514 (2009).
-

Supplemental Materials: Bound States in the Continuum in Compact Acoustic Resonators

WAVE EQUATION FOR THE DISPLACEMENT FIELD IN ISOTROPIC ELASTIC MEDIA.

Equation of motion for the elastic media can be written as [S1]

$$\rho \ddot{\mathbf{u}} = \nabla \cdot \hat{\boldsymbol{\sigma}}, \quad (\text{S1})$$

where ρ is the density of the media, \mathbf{u} is the displacement field and $\hat{\boldsymbol{\sigma}}$ is the Cauchy stress tensor. Stress tensor is connected with displacement field via the Hooke's law

$$\hat{\boldsymbol{\sigma}} = \hat{\mathbf{C}} : \hat{\boldsymbol{\varepsilon}}, \quad (\text{S2})$$

where $\hat{\mathbf{C}}$ is the fourth-rank tensor of the elastic constants and $\hat{\boldsymbol{\varepsilon}} = 1/2 [\nabla \mathbf{u} + (\nabla \mathbf{u})^T]$ is the infinitesimal strain tensor. In an isotropic elastic media, tensor of elastic constants is (in Voigt notation) [S2]

$$\hat{\mathbf{C}} = \begin{bmatrix} \lambda + 2\mu & \lambda & \lambda & 0 & 0 & 0 \\ & \lambda + 2\mu & \lambda & 0 & 0 & 0 \\ & & \lambda + 2\mu & 0 & 0 & 0 \\ & & & \mu & 0 & 0 \\ & & & & \mu & 0 \\ & & & & & \mu \end{bmatrix}, \quad (\text{S3})$$

or equivalently

$$C_{ijkl} = \lambda \delta_{ij} \delta_{kl} + \mu (\delta_{ik} \delta_{jl} + \delta_{jk} \delta_{il}), \quad (\text{S4})$$

thus giving the Hooke's law (S2) for isotropic media

$$\sigma_{ij} = \lambda \delta_{ij} \varepsilon_{kk} + 2\mu \varepsilon_{ij}. \quad (\text{S5})$$

Here λ and μ are the Lamé parameters. By substituting Hooke's law (S5) for isotropic media into the equation of motion (S1), and considering time-harmonic fields $\mathbf{u}(\mathbf{r}, t) \sim \mathbf{A}(\mathbf{r})e^{-i\omega t}$, one can obtain

$$\rho \omega^2 \mathbf{u} + (\lambda + 2\mu) \nabla \nabla \cdot \mathbf{u} - \mu \nabla \times \nabla \times \mathbf{u} = 0. \quad (\text{S6})$$

Using the Helmholtz theorem, displacement field can be expanded into the curl-free \mathbf{u}_s and divergence-free \mathbf{u}_p components

$$\begin{aligned} \mathbf{u} &= \mathbf{u}_s + \mathbf{u}_p, \\ \nabla \cdot \mathbf{u}_s &= 0, \nabla \times \mathbf{u}_p = 0. \end{aligned} \quad (\text{S7})$$

Substitution of the expansion Eq. (S7) into the Eq. (S6) with the help of the relation $\Delta = \nabla \nabla \cdot - \nabla \times \nabla \times$ will split equation (S6) into two equations. One for the pressure (curl-free) waves and one for the shear (divergence-free) waves

$$\Delta \mathbf{u}_i + k_i^2 \mathbf{u}_i = 0, \quad (\text{S8})$$

where index $i = p, s$ (pressure or shear), $k_i = \omega/c_i$ is the wavenumber of the pressure or shear wave, $c_p^2 = (\lambda + 2\mu)/\rho$, $c_s^2 = \mu/\rho$ are the speed of the pressure or shear wave in the media. One can see that equation (S8) is the Helmholtz equation.

CONNECTION BETWEEN PRESSURE AND DISPLACEMENT.

In the case of time-harmonic fields in nonviscous fluid (or gas) pressure $p(\mathbf{r})$ and velocity $\mathbf{v}(\mathbf{r})$ fields are connected as (in the first order of the perturbation theory) [S3]

$$\mathbf{v}(\mathbf{r}) = \frac{-i}{\rho_0 \omega} \nabla p(\mathbf{r}), \quad (\text{S9})$$

where ρ_0 is the density of the fluid. On the other hand, velocity is the time-derivative of the displacement $\mathbf{v}(\mathbf{r}) = \dot{\mathbf{u}}(\mathbf{r}) = -i\omega \mathbf{u}(\mathbf{r})$. Therefore,

$$\mathbf{u}(\mathbf{r}) = \frac{1}{\rho_0 \omega^2} \nabla p(\mathbf{r}). \quad (\text{S10})$$

VECTOR HARMONICS.

Vector harmonics are solutions of the vector Helmholtz equation and defined as follows [S4]

$$\mathbf{L} = \nabla\psi, \quad \mathbf{M} = \nabla \times (\mathbf{c}\psi), \quad \mathbf{N} = \frac{1}{k}\nabla \times \mathbf{M}, \quad (\text{S11})$$

where ψ is the solution of the scalar Helmholtz equation and \mathbf{c} is called direction vector. Since

1. \mathbf{M} and \mathbf{N} are the solutions of the Helmholtz equation

$$\nabla \times \mathbf{N} = \frac{1}{k}\nabla \times \nabla \times \mathbf{M} = k\mathbf{M}, \quad (\text{S12a})$$

2. \mathbf{M} and \mathbf{N} are solenoidal,

$$\nabla \cdot \mathbf{M} = \nabla \cdot \mathbf{N} = 0, \quad (\text{S12b})$$

3. \mathbf{L} is potential,

$$\nabla \times \mathbf{L} = 0. \quad (\text{S12c})$$

Spherical vector harmonics

In spherical system of coordinates (r, θ, φ) solution of the scalar Helmholtz equation can be written as

$$\psi_{\ell m}(\mathbf{r}, \mathbf{k}) = z_{\ell}(kr)P_{\ell}^m(\cos\theta)e^{im\varphi}, \quad (\text{S13})$$

where $z_{\ell}(x)$ is the spherical Bessel function of any kind. If one will take radius vector \mathbf{r} as a direction vector, one will get explicit view of vector spherical harmonics

$$\begin{aligned} \mathbf{L}_{\ell m}(\mathbf{r}, \mathbf{k}) &= \left[\hat{\mathbf{e}}_r \frac{\partial z_{\ell}(kr)}{\partial r} P_{\ell}^m(\cos\theta) + \hat{\mathbf{e}}_{\theta} \frac{z_{\ell}(kr)}{r} \frac{\partial P_{\ell}^m(\cos\theta)}{\partial \theta} + \hat{\mathbf{e}}_{\varphi} \frac{im}{r \sin\theta} z_{\ell}(kr) P_{\ell}^m(\cos\theta) \right] e^{im\varphi} \\ \mathbf{M}_{\ell m}(\mathbf{r}, \mathbf{k}) &= \left[\hat{\mathbf{e}}_{\theta} \frac{im}{\sin\theta} z_{\ell}(kr) P_{\ell}^m(\cos\theta) - \hat{\mathbf{e}}_{\varphi} z_{\ell}(kr) \frac{\partial P_{\ell}^m(\cos\theta)}{\partial \theta} \right] e^{im\varphi} \\ \mathbf{N}_{\ell m}(\mathbf{r}, \mathbf{k}) &= \left[\hat{\mathbf{e}}_r \frac{z_{\ell}(kr)}{kr} n(n+1) P_{\ell}^m(\cos\theta) + \hat{\mathbf{e}}_{\theta} \frac{1}{kr} \frac{\partial (r z_{\ell}(kr))}{\partial r} \frac{\partial P_{\ell}^m(\cos\theta)}{\partial \theta} + \hat{\mathbf{e}}_{\varphi} \frac{1}{kr} \frac{\partial (r z_{\ell}(kr))}{\partial r} \frac{im}{\sin\theta} P_{\ell}^m(\cos\theta) \right] e^{im\varphi} \end{aligned} \quad (\text{S14})$$

Cylindrical vector harmonics

In cylindrical system of coordinates (ρ, φ, z) solution of the scalar Helmholtz equation is

$$\psi_m(\mathbf{r}, \mathbf{k}) = Z_m(k_{\rho}\rho) e^{im\varphi} e^{ik_z z}, \quad (\text{S15})$$

where $Z_m(x)$ is the Bessel function of any kind. By taking the direction vector $\mathbf{c} = \hat{\mathbf{e}}_z$ and following definitions from the equation (S11), one can obtain explicit view of vector cylindrical harmonics

$$\begin{aligned} \mathbf{L}_m(\mathbf{r}, \mathbf{k}) &= \left[\hat{\mathbf{e}}_{\rho} \frac{\partial Z_m(k_{\rho}\rho)}{\partial \rho} + \hat{\mathbf{e}}_{\varphi} i \frac{m}{\rho} Z_m(k_{\rho}\rho) + \hat{\mathbf{e}}_z i k_z Z_m(k_{\rho}\rho) \right] e^{im\varphi} e^{ik_z z} \\ \mathbf{M}_m(\mathbf{r}, \mathbf{k}) &= \left[\hat{\mathbf{e}}_{\rho} i \frac{m}{\rho} Z_m(k_{\rho}\rho) - \hat{\mathbf{e}}_{\varphi} \frac{\partial Z_m(k_{\rho}\rho)}{\partial \rho} \right] e^{im\varphi} e^{ik_z z} \\ \mathbf{N}_m(\mathbf{r}, \mathbf{k}) &= \left[\hat{\mathbf{e}}_{\rho} i \frac{k_z}{k_{\rho}} \frac{\partial Z_m(k_{\rho}\rho)}{\partial \rho} - \hat{\mathbf{e}}_{\varphi} \frac{k_z}{k_{\rho}} \frac{m}{\rho} Z_m(k_{\rho}\rho) + \hat{\mathbf{e}}_z \frac{k_{\rho}^2}{k} Z_m(k_{\rho}\rho) \right] e^{im\varphi} e^{ik_z z} \end{aligned} \quad (\text{S16})$$

DERIVATION OF THE EIGENFREQUENCY EQUATION OF THE BICS IN A SPHERICAL RESONATOR

Because displacement field satisfies the Helmholtz equation (S8), it can be expanded using vector harmonics in a following manner

$$\mathbf{u}^{\text{in}}(\mathbf{r}) = \sum_i a_i \mathbf{M}_i(\mathbf{r}, \mathbf{k}_s) + b_i \mathbf{N}_i(\mathbf{r}, \mathbf{k}_s) + c_i \mathbf{L}_i(\mathbf{r}, \mathbf{k}_p), \quad (\text{S17a})$$

$$\mathbf{u}^{\text{out}}(\mathbf{r}) = \sum_i d_i \mathbf{L}_i^o(\mathbf{r}, \mathbf{k}_0), \quad (\text{S17b})$$

where, superscripts "in", "out" reflect the belonging of the field to the domain inside or outside of the resonator, $i = \{\ell, m\}$ for spherical vector harmonics and $i = m$ for cylindrical vector harmonics, \mathbf{k}_s and \mathbf{k}_p are the wavevectors of the shear and pressure modes respectively inside the resonator and \mathbf{k}_0 is the wavevector of the pressure waves in the surrounding fluid. Since fluid supports only purely longitudinal pressure waves, no \mathbf{M} and \mathbf{N} harmonics are present in the expansion (S17b) and index "o" at the longitudinal harmonic in the same expansion represents the fact that spherical Hankel $h_\ell^I(kr)$ or Hankel $H_m^I(k_\rho \rho)$ function is used to build the solution of the Helmholtz equation (equations (S13) and (S15)), while for the $\mathbf{M}(\mathbf{r}, \mathbf{k}_s)$, $\mathbf{N}(\mathbf{r}, \mathbf{k}_s)$ and $\mathbf{L}(\mathbf{r}, \mathbf{k}_p)$ harmonics in the expansion (S17a) spherical Bessel $j_\ell(kr)$ or Bessel $J_m(k_\rho \rho)$ function is taken as $z_\ell(kr)$ or $Z_m(k_\rho \rho)$. This choice was made on the basis of the following physical considerations

1. Field outside of the resonator is the outgoing wave $\Rightarrow z_\ell(kr) \& Z_m(k_\rho \rho) \rightarrow h_\ell^I(kr) \& H_m^I(k_\rho \rho)$,
2. Field inside of the resonator should be finite at the origin $\Rightarrow z_\ell(kr) \& Z_m(k_\rho \rho) \rightarrow j_\ell(kr) \& J_m(k_\rho \rho)$.

Using equation (S10) one can rewrite expansion of the field outside of the resonator (S17b) in terms of the pressure field

$$p^{\text{out}}(\mathbf{r}) = \sum_i \rho_0 \omega^2 d_i \psi_i^o(\mathbf{r}, \mathbf{k}_0), \quad (\text{S18})$$

For the solid-fluid interface boundary conditions are

$$\hat{\sigma}_{n\tau} = 0, \quad \hat{\sigma}_{nn} = -p^{\text{out}}, \quad u_n^{\text{in}} = u_n^{\text{out}}, \quad (\text{S19})$$

where indices n and τ denote components normal and tangential to the boundary respectively.

Consider a spherical acoustic resonator with radius a made of isotropic solid material immersed in a fluid. Due to the symmetry of the system, the spherical coordinate system will be the most convenient to use. In the spherical system of coordinates, strain tensor is written as [S1]

$$\begin{aligned} \varepsilon_{rr} &= \frac{\partial u_r}{\partial r}, & \varepsilon_{\theta\theta} &= \frac{1}{r} \frac{\partial u_\theta}{\partial \theta} + \frac{u_r}{r}, \\ \varepsilon_{\varphi\varphi} &= \frac{1}{r \sin \theta} \frac{\partial u_\varphi}{\partial \varphi} + \text{ctg } \theta \frac{u_\theta}{r} + \frac{u_r}{r}, & \varepsilon_{r\theta} &= \frac{1}{2} \left[\frac{1}{r} \frac{\partial u_r}{\partial \theta} + \frac{\partial u_\theta}{\partial r} - \frac{u_\theta}{r} \right], \\ \varepsilon_{r\varphi} &= \frac{1}{2} \left[\frac{1}{r \sin \theta} \frac{\partial u_r}{\partial \varphi} + \frac{\partial u_\varphi}{\partial r} - \frac{u_\varphi}{r} \right], & \varepsilon_{\theta\varphi} &= \frac{1}{2} \left[\frac{1}{r} \left(\frac{u_\varphi}{\partial \theta} - u_\varphi \text{ctg } \theta \right) + \frac{1}{r \sin \theta} \frac{\partial u_\theta}{\partial \varphi} \right]. \end{aligned} \quad (\text{S20})$$

One can show that

$$2\varepsilon_{r\theta} = \frac{\partial u_\theta}{\partial r} - \frac{u_\theta}{r} + \frac{1}{r} \frac{\partial u_r}{\partial \theta} = -\frac{1}{r} \left[r \frac{\partial u_\theta}{\partial r} + u_\theta \frac{\partial r}{\partial r} - \frac{\partial u_r}{\partial \theta} \right] + 2 \frac{\partial u_\theta}{\partial r} = -(\nabla \times \mathbf{u})_\varphi + 2 \frac{\partial u_\theta}{\partial r},$$

and

$$2\varepsilon_{r\varphi} = \frac{1}{r \sin \theta} \frac{\partial u_r}{\partial \varphi} + \frac{\partial u_\varphi}{\partial r} - \frac{u_\varphi}{r} = \frac{1}{r} \left[\frac{1}{\sin \theta} \frac{\partial u_r}{\partial \varphi} - r \frac{\partial u_\varphi}{\partial r} - u_\varphi \frac{\partial r}{\partial r} \right] + 2 \frac{\partial u_\varphi}{\partial r} = (\nabla \times \mathbf{u})_\theta + 2 \frac{\partial u_\varphi}{\partial r}.$$

Using equations (S5) and (S20) one can write boundary conditions (S19) for the boundary between solid sphere and fluid environment

$$1. \sigma_{r\theta} = 0$$

$$(\nabla \times \mathbf{u}^{\text{in}})_{\varphi} - 2 \frac{\partial u_{\theta}^{\text{in}}}{\partial r} = 0, \quad (\text{S21a})$$

$$2. \sigma_{r\varphi} = 0$$

$$(\nabla \times \mathbf{u}^{\text{in}})_{\theta} + 2 \frac{\partial u_{\varphi}^{\text{in}}}{\partial r} = 0, \quad (\text{S21b})$$

$$3. \sigma_{rr} = 0$$

$$\lambda \nabla \cdot \mathbf{u}^{\text{in}} + 2\mu \frac{\partial u_r^{\text{in}}}{\partial r} + p_{\text{out}} = 0, \quad (\text{S21c})$$

$$4. u_n^{\text{in}} = u_n^{\text{out}}$$

$$u_r^{\text{in}} = u_r^{\text{out}}. \quad (\text{S21d})$$

Substituting expansion (S17) into the boundary conditions (S21a) - (S21d) one will obtain set of equations for coefficients $a_{\ell m}$, $b_{\ell m}$, $c_{\ell m}$ and $d_{\ell m}$. Due to the orthogonality of the vector spherical harmonics, equations (S21a) - (S21d) should be satisfied for every ℓ and m separately. The equations (S21a) - (S21d) can be presented in the matrix form

$$\underbrace{\begin{bmatrix} k_s N_{\varphi} - 2\partial_r M_{\theta} & k_s M_{\varphi} - 2\partial_r N_{\theta} & -2\partial_r L_{\theta} & 0 \\ k_s N_{\theta} + 2\partial_r M_{\varphi} & k_s M_{\theta} + 2\partial_r N_{\varphi} & 2\partial_r L_{\varphi} & 0 \\ 0 & 2\mu\partial_r N_r & \lambda \operatorname{div} \mathbf{L} + 2\mu\partial_r L_r & \rho_0 \omega^2 \psi^o \\ 0 & N_r & L_r & -L_r^o \end{bmatrix}}_{\hat{\mathbf{D}}_{\ell m}} \underbrace{\begin{bmatrix} a \\ b \\ c \\ d \end{bmatrix}}_{\mathbf{f}_{\ell m}} \bigg|_{r=a} = 0, \quad (\text{S22})$$

where indices ℓ , m and arguments of the functions are omitted to improve readability. In order to bring the matrix $\hat{\mathbf{D}}_{\ell m}$ to a more noble form, let's take a look at its first two rows. Explicit view of these rows is

$$\begin{bmatrix} \frac{imr}{\sin \theta} \frac{\partial}{\partial r} \left(\frac{j_{\ell}^s}{r} \right) P_{\ell}^m & \frac{1}{k_s r^2} \frac{\partial P_{\ell}^m}{\partial \theta} \left[(2 - k_s^2 r^2) j_{\ell}^s + 2r \frac{\partial}{\partial r} \left(r \frac{\partial j_{\ell}^s}{\partial r} \right) \right] & 2 \frac{\partial}{\partial r} \left(\frac{j_{\ell}^p}{r} \right) \frac{\partial P_{\ell}^m}{\partial \theta} & 0 \\ r \frac{\partial}{\partial r} \left(\frac{j_{\ell}^s}{r} \right) \frac{\partial P_{\ell}^m}{\partial \theta} & \frac{-im}{k_s r^2} \frac{P_{\ell}^m}{\sin \theta} \left[(2 - k_s^2 r^2) j_{\ell}^s + 2r \frac{\partial}{\partial r} \left(r \frac{\partial j_{\ell}^s}{\partial r} \right) \right] & 2 \frac{-im}{\sin \theta} \frac{\partial}{\partial r} \left(\frac{j_{\ell}^p}{r} \right) P_{\ell}^m & 0 \end{bmatrix} e^{im\varphi}, \quad (\text{S23})$$

where arguments of $j_{\ell}(kr)$ and $P_{\ell}^m(\cos \theta)$ are omitted for the sake of brevity and indices s and p at the $j_{\ell}^{s,p}$ coincide with those of the wavevectors $k_{s,p}$ in the argument of the spherical Bessel function. By doing operations

$$\kappa_1 + \kappa_2 \frac{\sin \theta}{im} \frac{\partial_{\theta} P_{\ell}^m}{P_{\ell}^m} = \kappa'_1, \quad (\text{S24a})$$

$$\kappa_2 - \kappa'_1 \frac{m}{i \sin \theta} \frac{P_{\ell}^m \partial_{\theta} P_{\ell}^m}{m^2 \csc^2 \theta (P_{\ell}^m)^2 - (\partial_{\theta} P_{\ell}^m)^2} = \kappa'_2, \quad (\text{S24b})$$

where κ_1 and κ_2 are the rows of the matrix (S23), one can make the matrix $\hat{\mathbf{D}}_{\ell m}$ block-diagonal, and the solution of the matrix equation (S22) will be

$$\det \hat{\mathbf{D}}_{\ell m} = \underbrace{\det \hat{\mathbf{D}}_{\ell m}^{1 \times 1}}_{\text{BIC}} \cdot \underbrace{\det \hat{\mathbf{D}}_{\ell m}^{3 \times 3}}_{\text{Rad. modes}} = 0. \quad (\text{S25})$$

Therefore, matrix equation (S22) has two nontrivial solutions

$$\det \hat{\mathbf{D}}_{\ell m}^{1 \times 1} = 0, \quad \det \hat{\mathbf{D}}_{\ell m}^{3 \times 3} = 0, \quad (\text{S26})$$

where solution

$$\det \hat{\mathbf{D}}_{\ell m}^{1 \times 1} = -i \frac{r \sin \theta}{m P_{\ell}^m(\cos \theta)} \left[\frac{m^2}{\sin^2 \theta} (P_{\ell}^m(\cos \theta))^2 - \left(\frac{\partial P_{\ell}^m(\cos \theta)}{\partial \theta} \right)^2 \right] \frac{\partial}{\partial r} \left(\frac{j_{\ell}(k_s r)}{r} \right) e^{im\varphi} = 0 \quad (\text{S27})$$

is satisfies the matrix equation (S22) for $b = c = d = 0$ thus giving eigenfrequencies for BICs and can be rewritten as

$$(1 - \ell)j_{\ell}(x) + xj_{\ell+1}(x) = 0, \quad (\text{S28})$$

where $x = k_s a$. The roots of Eq. (S28) are shown in Table I.

TABLE I. First 3 roots of Eq. (S28) for BICs of the spherical resonator for $\ell = 1, 2, 3, 4$.

ℓ	1	2	3	4
x_1	5.76	2.50	3.86	5.09
x_2	9.10	7.13	8.44	10.51
x_3	12.32	10.51	11.88	13.21

ACOUSTIC BOUND STATES IN THE CONTINUUM IN A SOLID CYLINDRICAL RESONATOR

Since displacement field of BIC is completely localized in the resonator, eigenmode problem for BICs can be solved using stress-free boundary conditions

$$\hat{\sigma}_{n\tau} = 0, \quad \hat{\sigma}_{nn} = 0, \quad (\text{S29})$$

In cylindrical system of coordinates components of the Cauchy stress tensor are presented as [S1]

$$\begin{aligned} \varepsilon_{\rho\rho} &= \frac{\partial u_{\rho}}{\partial \rho}, & \varepsilon_{\varphi\varphi} &= \frac{1}{\rho} \frac{\partial u_{\varphi}}{\partial \varphi} + \frac{u_{\rho}}{\rho}, & \varepsilon_{zz} &= \frac{\partial u_z}{\partial z}, \\ \varepsilon_{\varphi z} &= \frac{1}{2} \left[\frac{1}{\rho} \frac{\partial u_z}{\partial \varphi} + \frac{\partial u_{\varphi}}{\partial z} \right], & \varepsilon_{\rho z} &= \frac{1}{2} \left[\frac{\partial u_{\rho}}{\partial z} + \frac{\partial u_z}{\partial \rho} \right], & \varepsilon_{\rho\varphi} &= \frac{1}{2} \left[\frac{\partial u_{\varphi}}{\partial \rho} - \frac{u_{\varphi}}{\rho} + \frac{1}{\rho} \frac{\partial u_{\rho}}{\partial \varphi} \right], \end{aligned} \quad (\text{S30})$$

where non-diagonal components can be reduced to the following form

$$2\varepsilon_{\rho\varphi} = \frac{1}{\rho} \left(-\rho \frac{\partial u_{\varphi}}{\partial \rho} - u_{\varphi} \frac{\partial \rho}{\partial \rho} + \frac{\partial u_{\rho}}{\partial \varphi} \right) + 2 \frac{\partial u_{\varphi}}{\partial \rho} = -(\nabla \times \mathbf{u})_z + 2 \frac{\partial u_{\varphi}}{\partial \rho},$$

$$2\varepsilon_{\rho z} = \frac{\partial u_{\rho}}{\partial z} - \frac{\partial u_z}{\partial \rho} + 2 \frac{\partial u_z}{\partial \rho} = (\nabla \times \mathbf{u})_{\varphi} + 2 \frac{\partial u_z}{\partial \rho}.$$

Hereby explicit form of boundary conditions is

- At the side surface of the cylinder - for $\rho = a$

$$1. \quad \sigma_{\rho\varphi} = 0$$

$$-(\nabla \times \mathbf{u})_z + 2 \frac{\partial u_{\varphi}}{\partial \rho} = 0, \quad (\text{S31a})$$

$$2. \quad \sigma_{\rho z} = 0$$

$$(\nabla \times \mathbf{u})_{\varphi} + 2 \frac{\partial u_z}{\partial \rho} = 0, \quad (\text{S31b})$$

$$3. \quad \sigma_{\rho\rho} = 0$$

$$\lambda \nabla \cdot \mathbf{u} + 2\mu \frac{\partial u_{\rho}}{\partial \rho} = 0, \quad (\text{S31c})$$

- On the bases of the cylinder - for $z = \pm h/2$

1. $\sigma_{z\varphi} = 0$

$$(\nabla \times \mathbf{u})_\rho + 2 \frac{\partial u_\varphi}{\partial z} = 0, \quad (\text{S32a})$$

2. $\sigma_{z\rho} = 0$

$$(\nabla \times \mathbf{u})_\varphi + 2 \frac{\partial u_z}{\partial \rho} = 0, \quad (\text{S32a})$$

3. $\sigma_{zz} = 0$

$$\lambda \nabla \cdot \mathbf{u} + 2\mu \frac{\partial u_z}{\partial z} = 0, \quad (\text{S32c})$$

where a and h are the radius and height of the cylindrical resonator, respectively. Before proceeding, it is important to make a few notes that will simplify the mathematical calculations.

1. Due to the symmetry of the cylinder only modes with azimuthal number $m = 0$ will be the BICs [S5]. This can be also understood from the explicit view of the \mathbf{M}_m vector cylindrical harmonic (S16), since it has nonzero radial component for $m \neq 0$.
2. Vector cylindrical harmonics generated using $\psi(\mathbf{r}) = \psi(\rho, \varphi) e^{ik_z z}$ will not satisfy boundary conditions for the bases of the cylinder since $e^{ix} \neq 0$ for $x \in \mathbb{R}$, therefore, basis of the standing waves should be used

$$\psi_m(\mathbf{r}, \mathbf{k}) = J_m(k_\rho \rho) [A^o \sin(k_z z) + A^e \cos(k_z z)] e^{im\varphi}, \quad (\text{S33})$$

where indices "o" and "e" near the amplitudes A^o and A^e reflect the odd or even nature of the sine and cosine relative to zero.

3. All harmonics with different azimuthal number m and parity $q = o, e$ are fully decoupled and therefore can be considered separately.

Considering all the comments above, the decomposition of the displacement field is written as

$$\mathbf{u}_0^q(\mathbf{r}) = a^q \mathbf{M}_0^q(\mathbf{r}, \mathbf{k}_s) + b^q \mathbf{N}_0^q(\mathbf{r}, \mathbf{k}_s) + c^q \mathbf{L}_0^q(\mathbf{r}, \mathbf{k}_p). \quad (\text{S34})$$

By direct substitution of the expansion (S34) into the boundary conditions (S31a) - (S32c) one can obtain two matrix equations

$$\underbrace{\begin{bmatrix} 2\partial_\rho M_\varphi - k_s N_z & 0 & 0 \\ 0 & 2\partial_\rho N_z + k_s M_\varphi & 2\partial_\rho L_z \\ 0 & 2\mu\partial_\rho N_\rho & \lambda\Delta\psi_p + 2\mu\partial_\rho L_\rho \end{bmatrix}}_{\mathbf{D}_m^\rho} \underbrace{\begin{bmatrix} a \\ b \\ c \end{bmatrix}}_{\mathbf{f}_m^\rho} \bigg|_{\rho=a} = 0 \quad (\text{S35})$$

for the side surface of the cylinder and

$$\underbrace{\begin{bmatrix} 2\partial_z M_\varphi + k_s N_\rho & 0 & 0 \\ 0 & 2\partial_\rho N_z + k_s M_\varphi & 2\partial_\rho L_z \\ 0 & 2\mu\partial_z N_z & \lambda\Delta\psi_p + 2\mu\partial_z L_z \end{bmatrix}}_{\mathbf{D}_m^z} \underbrace{\begin{bmatrix} a \\ b \\ c \end{bmatrix}}_{\mathbf{f}_m^z} \bigg|_{z=\pm h/2} = 0 \quad (\text{S36})$$

for the bases of the cylinder. Indices 0, q and arguments of the functions in the equations (S35) and (S36) are omitted for the sake of brevity. One of solutions of matrix equations (S35) and (S36), which corresponds to the BIC is

$$\begin{cases} 2\partial_\rho M_\varphi - k_s N_z \big|_{\rho=a} = 0, \\ 2\partial_z M_\varphi + k_s N_\rho \big|_{z=\pm h/2} = 0. \end{cases} \quad (\text{S37})$$

Explicitly, the equations (S37) can be written as

$$\underbrace{\begin{cases} J_2(k_\rho a) = 0, \\ \cos(k_z h/2) = 0, \end{cases}}_{\text{odd mode}} \quad \underbrace{\begin{cases} J_2(k_\rho a) = 0, \\ \sin(k_z h/2) = 0, \end{cases}}_{\text{even mode}} \quad (\text{S38})$$

thus giving k_ρ and k_z components of the wavevector of the odd or even BICs. Eigenfrequencies of the BICs can be calculated as

$$\omega^2 = c_t^2 \left[\left(\frac{\alpha_n}{a} \right)^2 + \left(\frac{\pi q}{h} \right)^2 \right], \quad (\text{S39})$$

where α_n is the n 'th root of the Bessel function of the second order $J_2(x)$, and $q = \pm 1, \pm 3, \pm 5 \dots$ for the odd and $0, \pm 2, \pm 4 \dots$ for the even modes.

CLASSIFICATION OF THE MODES IN SOLIDS OF $D_{\infty h}$ SYMMETRY

TABLE II. Multipole content and classification of eigenmodes, and selection rules for eigenmode excitation by a plane wave in the objects of $D_{\infty h}$ symmetry (spheroid, cylinder, symmetrical dimer etc).

Irrep	Degree of degeneracy	Mode	Azimuthal number	Parity	Multipoles	Excitation along x or y	Excitation along z	Excitation at oblique incidence
A_{1u}	1	Radiative mode	$m = 0$	odd	$\mathbf{L}_{1,0}, \dots, \mathbf{L}_{2s+1,0}$ $\mathbf{N}_{1,0}, \dots, \mathbf{N}_{2s+1,0}$	No	Yes	Yes
A_{1g}	1	Radiative mode	$m = 0$	even	$\mathbf{L}_{0,0}, \dots, \mathbf{L}_{2s,0}$ $\mathbf{N}_{2,0}, \dots, \mathbf{N}_{2s,0}$	No	Yes	Yes
A_{2g}	1	BIC	$m = 0$	even	$\mathbf{M}_{1,0}, \dots, \mathbf{M}_{2s+1,0}$	No	No	No
A_{2u}	1	BIC	$m = 0$	odd	$\mathbf{M}_{2,0}, \dots, \mathbf{M}_{2s,0}$	No	No	No
E_{1g}	2	Radiative mode	$m = \pm 1$	odd	$\mathbf{L}_{2,\pm 1}, \dots, \mathbf{L}_{2s,\pm 1}$ $\mathbf{N}_{2,\pm 1}, \dots, \mathbf{N}_{2s,\pm 1}$ $\mathbf{M}_{1,\pm 1}, \dots, \mathbf{M}_{2s+1,\pm 1}$	No	No	Yes
E_{1u}	2	Radiative mode	$m = \pm 1$	even	$\mathbf{L}_{1,\pm 1}, \dots, \mathbf{L}_{2s+1,\pm 1}$ $\mathbf{N}_{1,\pm 1}, \dots, \mathbf{N}_{2s+1,\pm 1}$ $\mathbf{M}_{2,\pm 1}, \dots, \mathbf{M}_{2s,\pm 1}$	Yes	No	Yes
E_{2u}	2	Radiative mode	$m = \pm 2$	odd	$\mathbf{L}_{3,\pm 2}, \dots, \mathbf{L}_{2s+1,\pm 2}$ $\mathbf{N}_{3,\pm 2}, \dots, \mathbf{N}_{2s+1,\pm 2}$ $\mathbf{M}_{2,\pm 2}, \dots, \mathbf{M}_{2s,\pm 2}$	No	No	Yes
E_{2g}	2	Radiative mode	$m = \pm 2$	even	$\mathbf{L}_{2,\pm 2}, \dots, \mathbf{L}_{2s,\pm 2}$ $\mathbf{N}_{2,\pm 2}, \dots, \mathbf{N}_{2s,\pm 2}$ $\mathbf{M}_{3,\pm 2}, \dots, \mathbf{M}_{2s+1,\pm 2}$	Yes	No	Yes
E_{3g}	2	Radiative mode	$m = \pm 3$	odd	$\mathbf{L}_{4,\pm 3}, \dots, \mathbf{L}_{2s,\pm 3}$ $\mathbf{N}_{4,\pm 3}, \dots, \mathbf{N}_{2s,\pm 3}$ $\mathbf{M}_{3,\pm 3}, \dots, \mathbf{M}_{2s+1,\pm 3}$	No	No	Yes
E_{3u}	2	Radiative mode	$m = \pm 3$	even	$\mathbf{L}_{3,\pm 3}, \dots, \mathbf{L}_{2s+1,\pm 3}$ $\mathbf{N}_{3,\pm 3}, \dots, \mathbf{N}_{2s+1,\pm 3}$ $\mathbf{M}_{4,\pm 3}, \dots, \mathbf{M}_{2s,\pm 3}$	Yes	No	Yes
\vdots	\vdots	\vdots	\vdots	\vdots	\vdots	\vdots	\vdots	\vdots

Table II shows the classification of eigenmodes in solids of $D_{\infty h}$ symmetry (spheroid, cylinder, symmetrical dimer etc). We assume that the rotation axis is the z -axis. As the considered bodies of revolution have a mirror symmetry with respect to the xy -plane, we can define a parity of the modes under transformation $z \rightarrow -z$ as follows

$$\begin{bmatrix} u_\rho(\rho, \varphi, -z) \\ u_\varphi(\rho, \varphi, -z) \\ u_z(\rho, \varphi, -z) \end{bmatrix} = \sigma_z \begin{bmatrix} u_\rho(\rho, \varphi, z) \\ u_\varphi(\rho, \varphi, z) \\ -u_z(\rho, \varphi, z) \end{bmatrix}. \quad (\text{S40})$$

If $\sigma_z = 1$ then the mode is defined as even, and if $\sigma_z = -1$ then the mode is defined as odd.

* ilya.deriya@metalab.itmo.ru

† a.bogdanov@metalab.itmo.ru

[S1] L. D. Landau and E. M. Lifshitz. *Theory of elasticity*. Pergamon, 1959.

[S2] John Frederick Nye et al. *Physical properties of crystals: their representation by tensors and matrices*. Oxford university press, 1985.

[S3] Henrik Bruus. Acoustofluidics 2: Perturbation theory and ultrasound resonance modes. *Lab on a Chip*, 12(1):20–28, 2012.

[S4] Craig F Bohren and Donald R Huffman. *Absorption and scattering of light by small particles*. John Wiley & Sons, 2008.

[S5] Sergey Gladyshev, Kristina Frizyuk, and Andrey Bogdanov. Symmetry analysis and multipole classification of eigenmodes in electromagnetic resonators for engineering their optical properties. *Phys. Rev. B*, 102(7):075103, 2020.